

# Scale Invariant Semantic Segmentation with RGB-D Fusion

Mohammad Dawud Ansari<sup>1</sup>, Alwi Husada<sup>2</sup> and Didier Stricker<sup>1</sup>

**Abstract**—In this paper, we propose a neural network architecture for scale-invariant semantic segmentation using RGB-D images. We utilize depth information as an additional modality apart from color images only. Especially in an outdoor scene which consists of different scale objects due to the distance of the objects from the camera. The near distance objects consist of significantly more pixels than the far ones. We propose to incorporate depth information to the RGB data for pixel-wise semantic segmentation to address the different scale objects in an outdoor scene. We adapt to a well-known DeepLab-v2(ResNet-101) model as our RGB baseline. Depth images are passed separately as an additional input with a distinct branch. The intermediate feature maps of both color and depth image branch are fused using a novel fusion block. Our model is compact and can be easily applied to the other RGB model. We perform extensive qualitative and quantitative evaluation on a challenging dataset Cityscapes. The results obtained are comparable to the state-of-the-art. Additionally, we evaluated our model on a self-recorded real dataset. For the sake of extended evaluation of a driving scene with ground truth we generated a synthetic dataset using popular vehicle simulation project CARLA. The results obtained from the real and synthetic dataset shows the effectiveness of our approach.

## I. INTRODUCTION

Deep Convolutional Neural Networks (DCNNs) have shown remarkable accuracy for computer vision tasks like object classification [5]–[8] and object detection [9]–[13]. In the era of autonomous driving, classification and detection are not sufficient informations that can guide a vehicle in an unknown environment autonomously. As an example, such a system must be able to detect pedestrian from car and house and so on.

In Computer Vision community applies for this task dense per-pixel classification called as pixel-wise semantic segmentation. The goal of semantic segmentation is to recognize and understand which pixels level belong to which object in the image. Semantic segmentation gives benefits to various applications such as robotic vision, autonomous cars, medical imaging data [14] etc. Earlier approaches [2]–[4], [15], [16] provide reasonable accuracy. However, this task is difficult with implicit problems such as illuminations, occlusions, cluttered background and multi-scale of objects.

Earlier multi-scale problem is solved by employing a network which takes input images with multiple resolutions and later aggregates the feature maps [17]–[19]. Since the computation is performed parallelly for different scale, the overall computation cost is higher, in terms of memory

requirement and computation power. Other alternatives to solve multi-scale problem are proposed by [4], [16]. Depth information can help to solve the problem of ambiguity in the scale [3]. Additionally, contextual information can be obtained by parallel pyramid pooling network as proposed in [15]. We merge multi-scale feature generation along with contextual information and the depth information to tackle the problem of scale in driving scenes. We summarize the contributions of the paper as follows:

- We propose a new depth branch which takes the input as a raw depth image. The input layer of the neural network is modified to accept single channel input. Additionally, the resolution of diminishing activation map is retained similar to RGB branch utilizing dilated convolution. The intermediate full resolution feature maps from depth branch are merged with the RGB branch using a novel fusion block. Depth information resolves the ambiguity in scale change of similar objects.
- We describe a scale-invariant pyramid pooling neural network model for semantic segmentation, which can cope with difficult scale changes for similar objects. Smaller dilation rate is used in every level of the pyramid pooling network which majorly focuses on the smaller objects. However, to maintain the invariance for bigger objects, we adapt Global Average Pooling, which is also essential to keep the contextual information.
- We describe a simple generation and utilization of a synthetic dataset with ground truth using vehicle simulation project CARLA [20]. An additional dataset with ground truth can be used to increase invariance in the neural network, and for extensive non-biased evaluation.
- An extensive quantitative evaluation is performed on Cityscapes [21] and synthetic driving dataset CARLA [20]. Additionally, we perform the qualitative evaluation on a self-generated real Zed dataset. The results obtained using our proposed model are promising for difficult scale changes of the similar object, which is also comparable to the state-of-the-art.

## II. RELATED WORKS

Over the past few years, the breakthroughs of Deep Learning in images classification were quickly transferred into the semantic segmentation task. The introduction of Fully Convolutional Network [1] which modifies the last fully connected layer to spatial output. This enables for solving pixel-wise semantic segmentation that required the output label map to have same spatial size as the input. The

<sup>1</sup>German Research Center for Artificial Intelligence (DFKI GmbH), Germany. {dawudmaxx@gmail.com, didier.stricker@dfki.de}

<sup>2</sup>University of Kaiserslautern, Germany. husada@rhrk.uni-kl.de

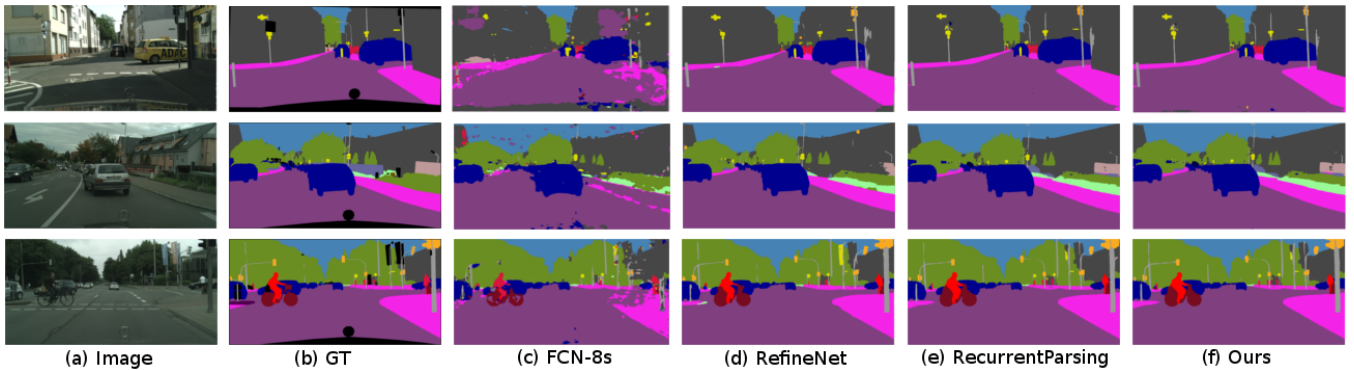


Fig. 1. Qualitative results of our model compared to FCN-8s [1], RefineNet [2], RecurrentParsing [3] and DeepLab-v2(ResNet-101)[4] on Cityscapes dataset (validation set).

issues in the deep fully convolutional network is a set of stride in convolution and maximum/average pooling. These operations downsample the spatial size of feature maps, causing the diminishing response. Several approaches have been proposed to remedy the issue. Shelhamer *et al.* [1] upsample the feature maps from top layers and concatenate it with the feature maps from intermediate layers. Eigen and Fergus [22] cascade multi-scale Deep Convolutional Neural Network (DCNN). They concatenate fine-details result with the coarse input and use it as an input to the next DCNN. Noh *et al.* [23], use encoder-decoder architecture. They apply deconvolution also known as transposed convolution in the decoder part.

Another approach is proposed by Chen *et al.* [4], which we use as a baseline. This method is referred as DeepLab-v2(ResNet-101). They introduce "atrous convolution" to adjust receptive fields size by inserting "hole" in the filter. It expands the receptive field without adding extra parameters. A paper from Wang *et al.* [24] proposed different method to upsample spatial size of the top feature maps. Instead of using deconvolution [1], [23] or bilinear interpolation [3], [16], they introduce Dense Upsampling Convolution (DUC), in which they arrange the top layer shape to have multiple channels of label map.

Several Deep Convolution Neural Network (DCNN) models are proposed which combines depth information with color information for semantic segmentation [25]–[27]. The fusion strategy affects the overall accuracy of the model. We experiment our model with different fusion strategy and use the optimal one. Hazirbas *et al.* [25] proposed an encoder-decoder type model that use two branches in encoder part to extract feature maps of RGB and depth images separately. They sum both feature maps which is later fed to the decoder part to get the final prediction. We adapt similar methodology in our approach with additional modifications. Cheng *et al.* [27] introduces a gated fusion method. It consists of concatenation, convolution and sigmoid layer. They concatenated the top feature maps from RGB and depth branch, and then the resulting features are convolved with  $3 \times 3$  filters followed by sigmoid layer to regularize the features. The outputs of sigmoid are used to weigh the contribution of

depth and RGB features. Park *et al.* [26] extends RefineNet [2] architecture to integrate depth information. They propose Multi-modal Feature Fusion (MMF), which composed of the same component as RefineNet block but it accepts RGB and depth feature maps as inputs. Kong and Fowlkes [3] proposed another direction of incorporating depth information to the RGB-based model. Instead of using different branches for feature extraction, their approach estimates depth information, and it then used for gating the size of pooling field in convolution model. They trained their gating method with Recurrent Neural Network (RNN) strategy. Our work is motivated by the gating mechanism as it resembles size invariance in the feature maps. This is useful for generating intermediate feature maps which are scale invariant.

### III. PROPOSED ARCHITECTURE

The proposed model architecture is motivated from DeepLab-v2(ResNet-101) [4]. This model has two major parts. The first part is referred as ResNet-101 [28] for feature maps generation and the second part is referred as Pyramid Pooling. This combined network is named Atrous Spatial Pyramid Pooling (ASPP). Our model can be seen in Figure 2. In contrast to DeepLab-v2(ResNet-101) [4] our model has a parallel branch that accepts depth image as input. The features are generated from color as well as depth image separately. We then combine feature maps from both branches in the fusion block, which is passed to the ASPP and later to final prediction. The ASPP consists of five parallel convolutions + Batch Normalization + ReLU blocks with different dilation rate.

#### A. RGB-D Architecture

We will briefly review DeepLab-v2(ResNet-101) architecture proposed by [4]. One implicit problem in Deep Convolution Neural Network (DCNN) for Semantic Segmentation is consecutive maximum/average pooling and striding in convolutions operation that reduce spatial input dimension into significantly smaller feature maps. This downsample factor is about 32 with the actual input dimension. To overcome this issue Chen *et al.* [4] proposed 'atrous' convolution also known as dilated convolution. The output signal  $o\{i\}$

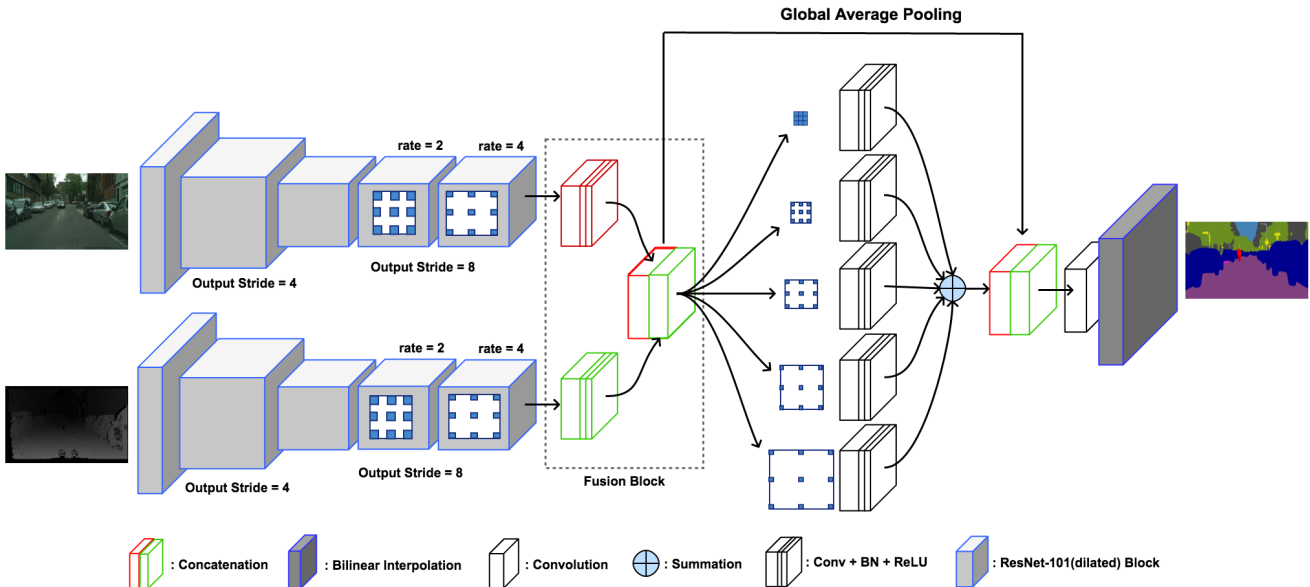


Fig. 2. Overview of our proposed architecture. The model mainly composed of two branches of features generation, Fusion Block Layer and Pyramid Pooling. We use Atrous ResNet-101 to extract robust features from both RGB and depth images. We then combine feature maps from both branches in the Fusion Block, which is passed to the Pyramid Pooling and later to final prediction. Additionally, Global Average Pooling is applied to get contextual information.

obtained after applying a dilated convolution in a 1D signal is given as:

$$o[i] = \sum_{l=1}^L x[i + r \cdot l]f[l], \quad (1)$$

where  $x[i]$  is an input signal,  $f[l]$  is a filter that has length  $L$  and  $r$  is a dilation rate. Noting that, when  $r = 1$  is a standard convolution. In a 2D convolutional operation, atrous convolution can be seen as inserting 'hole' to the convolution filter (inserting zeros between two neighboring pixels in the filter). By defining the dilation rate  $r$ , it allows us to modify the size of receptive fields without changing the filter size. In addition, it also lets us control the spatial output size of feature maps of convolutions operation. In DeepLab-v3 [16] the spatial output size of feature maps is denoted as  $output\_stride$ , which can also be termed as the reduction factor of the spatial input size to produce the desired output. For example, in original ResNet-101 model, the  $output\_stride$  is 32 [28]. In order to obtain a bigger spatial dimension of the output feature maps, assuming the  $output\_stride$  to be 16, the stride of the last pooling and convolution layer is set to 1 and modify the dilation rate of the subsequent convolution layers to 2. The feature maps from the last ResNet-101 layer are fed to the Atrous Spatial Pyramid Pooling (ASPP). It consists of several parallel filters with different dilation rate to exploit different scale of features. In DeepLab-v2(ResNet-101) [4], the ASPP composed of four different filters with dilation rate  $\{6, 12, 18, 24\}$ . They are summed together before upsampled by  $output\_stride$  factor with bilinear interpolation.

In our model, we use  $output\_stride = 8$ . The repetitive convolution operation causes the diminishing of size of the

features maps. An alternative to this operation is the use of  $output\_stride = 1$  along with dilation rate and modifying the stride of all the convolution layer to obtain same size feature maps. However, this operation is costly in terms of memory and training time. Thus  $output\_stride = 8$  is a reasonable choice to deal with the trade-off between memory usage and accuracy. This is the reason for setting the  $output\_stride = 8$  in our model. To handle depth data, we add an additional dilated ResNet-101 [28] branch with  $output\_stride = 8$ . We modify the first convolution layer to accept one channel image instead of three channels (RGB). The rest of the layers in depth branch are same as its RGB counterpart. The explanation of this part of the model is shown in Figure 2.

### B. Fusion Block

One trivial way to integrate depth information into existing RGB-based model, is by stacking both images as a single 4-channel RGB-D image and modifying the first convolution layer to accept a 4-channel input [29]. Furthermore, Hazirbas *et al.* [25] showed that stacking RGB-D input produces less discriminant features than when fusing RGB and depth feature maps. The intuitive idea of fusing RGB and depth feature maps can be seen in the term of neuron-wise activation. For a given pixel, the activation maps from color and depth branch complement each other simultaneously thereby producing more accurate segmentation. Motivated from this idea along with Hazirbas *et al.* [25] we propose fusion block which is composed by convolution followed by summation or concatenation. Given feature maps of RGB and depth from the last Atrous ResNet-101 with dimension  $H \times W \times 2048$  where  $H$  and  $W$  are height and width of the feature maps,

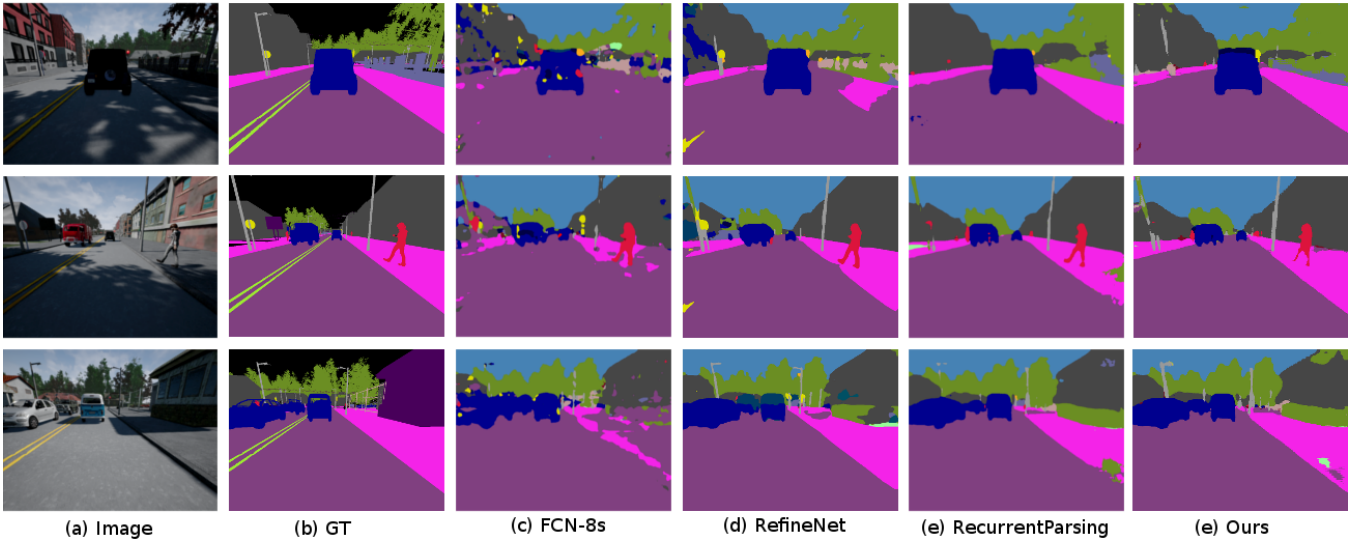


Fig. 3. Qualitative results of our model compared to FCN-8s [1], RefineNet [2], RecurrentParsing [3] and DeepLab-v2(ResNet-101)[4] on CARLA dataset.

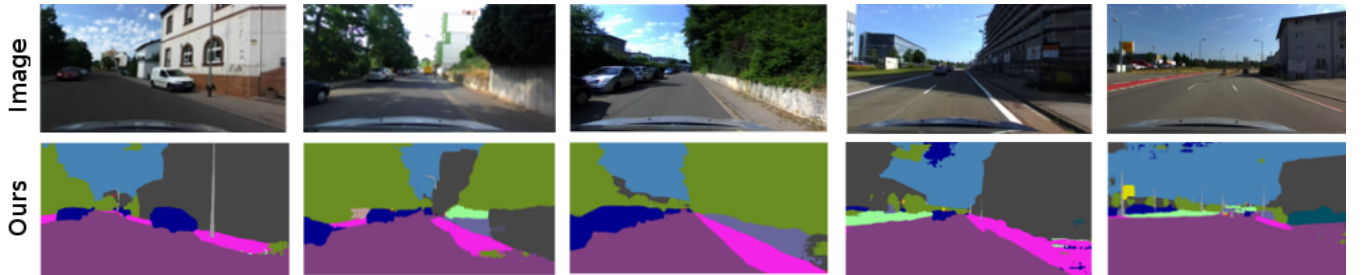


Fig. 4. Qualitative results of our model on self-recorded Zed dataset.

we reduce the dimension to be  $H \times W \times 512$ . We then fuse both feature maps to get more discriminant features representation, which are then fed to the pyramid pooling network. We experiment with sum and concatenation for fusing the feature maps. The results show that concatenation produce better accuracy. The explanation of this part of the model is shown in Figure 2.

### C. Pyramid Pooling

Many earlier approaches were proposed which provides significant accuracy with single object without much variation in the object’s scale [1], [23], [25]. This creates an implicit issue for segmenting multi-scale objects in a scene. Especially small objects which are far away from the camera. Motivated from [4], [25], we intend to solve this issue by incorporating depth information and applying pyramid pooling. In contrast, we apply five parallel convolutions + Batch Normalization + ReLU blocks with different dilation rate. We modified  $2^{nd}$  till  $5^{th}$  pyramid level convolution operations with  $3 \times 3$  filters with dilation rate  $\{2, 4, 8, 16\}$  respectively. The  $1^{st}$  pyramid level convolution operation uses  $1 \times 1$  filters without dilation rate as in [16]. With small dilation rate the contextual information from the scene is lost as stated in [4], [15], [16]. As a turn around, we employ global average pooling [15] which can retain

the contextual information making the feature maps more responsive with context to nearby objects (eg. pedestrian near grass or a pedestrian near a car). The input of fusion block is fed to global average pooling which generated the average feature maps. We employ summation to merge the outputs of all pyramid level convolution operations. The outputs from pyramid pooling and global average pooling are concatenated, and the resulting features is passed to  $1 \times 1$  convolution to produce final *logits* (class-wise probabilistic map along the depth channel of the feature map). We use bilinear interpolation of *logits* to get full resolution for our prediction maps. The combination of dilation rate  $\{2, 4, 8, 16\}$ , global average pooling along with fusion from the depth branch, we have proven that our results are better when recognizing small objects compared to other methods. This can be verified from the quantitative and qualitative evaluations in the Section IV.

To summarize, our propose model consists of four parts. First part is feature extractors which is composed by two branches of Atrous ResNet-101 to extract features of RGB and depth images. Second part is fusion block that fuses feature maps from both RGB and depth. Third part is global average pooling which is useful to retain the contextual information in the feature maps. The last part consists of

pyramid pooling and final prediction. The pyramid pooling is composed of five convolution layers that are arranged in a parallel order.

#### D. Implementation Details

We use pre-trained ResNet-101 [28] on ImageNet [30] for feature maps generation in RGB and depth branches separately. The original ResNet-101 requires three channels (RGB) image as an input. Therefore, in our depth branch, we modify the first convolution layer to accept one channel image. We initialize the weights for the first convolution layer in depth branch by averaging the weights of the first convolution layer in RGB branch along the channel dimension. In contrast with the original ResNet-101 [28] we remove the first  $7 \times 7$  convolution layer and change to three  $3 \times 3$  convolution layers as in [3], [24]. This modification keeps the receptive field similar to additional parameters to learn and makes the network deeper. We adjust the  $output\_stride = 8$  by adding  $dilation\ rate = 2$  and  $rate = 4$  in the last two residual blocks (res4 and res5 in our naming notation) respectively (see Figure 2). We upsample the top-most feature maps with bilinear interpolation by a factor of eight to make the final prediction of full resolution. Our implementation is built on top of the open-source code provided by Kong and Fowlkes [3] which uses MatConvNet [31] framework.

#### E. Training Protocol

We train our models with the following procedure: Initially, we train RGB and depth branch separately. We insert fusion block before pyramid pooling to combine feature maps generated from both Atrous ResNet-101 from the RGB and depth trained models, which is then passed to pyramid pooling and later for final prediction. Finally, we freeze Atrous ResNet-101 for training Fusion Block and Pyramid Pooling to get our final prediction. This is achieved by setting the learning rate of the freezing layers to zero.

We employ "poly" learning rate policy, in which a base learning rate is multiplied by  $(1 - \frac{iter}{maxiter})^{momentum}$ . We set the base learning rate to  $5 \times 10^{-5}$  and  $momentum = 0.9$ . Due to limited GPU memory and large image resolution, we set the batch size to one. Atrous convolution requires large cropping size to make dilation rate effective [16]. Therefore, we randomly crop the input images to  $720 \times 720$  during training on Cityscapes [21]. We set the momentum to 0.9 and weight decay to 0.0005. For data augmentation, we randomly scale the cropped input images with the scale rate between 0.5 and 2.0 and also perform left-right flipping. In the case of training for the RGB model, we also add color jittering. We trained our model for total 200 epochs. From epoch 140 onwards, we change the base learning rate to  $5 \times 10^{-4}$  and weight decay of pyramid pooling layers to 0.999.

### IV. EXPERIMENTAL EVALUATION

We evaluate our model on Cityscapes [21]. It is a large-scale outdoor scene dataset recorded across 50 German cities with different seasons, i.e. spring, summer, and fall.

The dataset contains RGB-D pairs of 2975 (*train*), 500 (*validation*) and 1525 (*test*) image sets with pixel-wise *fine-annotation* labels. Additionally, 20000 extra train RGB-D image pairs with *coarse-annotation* labels is provided. We also evaluate on synthetic dataset generated from a publicly available driving simulation framework CARLA [20]. CARLA is an open-source simulator for self-driving car, built on Unreal Engine 4 (UE4) [32]. We generated 5000 (*train*) and 500 (*validation*) RGB-D pairs image sets. Furthermore, we perform qualitative evaluation on our self-recorded real data Zed dataset. We captured Zed dataset using a front-facing zed stereo camera [33] mounted on a car.

We provide our quantitative results on *test* data for Cityscapes and *validation* data for CARLA. We did adjustments in class mapping for CARLA quantitative measurement as follows: First, we ignored two classes, i.e. *road line* and *others*, because they do not exist in Cityscapes. Then we grouped *car*, *truck* and *bus* classes from Cityscapes to the *vehicles* class in CARLA. Other classes from Cityscapes that do not exist in CARLA are set to *unlabeled* and ignored in IoU measurement. We compare our results to other well-known approaches such as FCN-8s [1], RefineNet [2], RecurrentParsing [3], DeepLab-v2(ResNet-101) [4] and PSPNet [15]. We used intersection-over-union (*IoU*)<sup>1</sup> metric for quantitative evaluation. We average the IoU result across 10 classes for CARLA [20] and 19 classes for Cityscapes [21].

#### A. Qualitative

In Figure 1, we compare our qualitative results on Cityscapes [21] with the ground truth and other methods. It can be seen that our segmentation is close to ground truth. In comparison to others, we can see that our segmentation stands out of the FCN-8s [1]. Compare to RefineNet [2], we perform better in segmenting narrow *building* and far distant *pole* that can be seen in the 1<sup>st</sup> row.

In Figure 3, we compare our qualitative results on CARLA [20] with the ground truth and other methods. In rows 1<sup>st</sup> – 3<sup>rd</sup>, our approach correctly segments *side walk* where other methods fail. Furthermore, our model correctly segments other objects in the scenes such as *pedestrians*, *cars*, *roads*, *buildings* and *vegetation*. One fail case of our segmentation is in 1<sup>st</sup> row, where it fails to segment *poles* and *traffic sign* nearby the buildings. It can be because of the same texture and color of the poles with the nearby buildings. Another visual difference from our result with the ground truth is the *sky* segmentation. In all prediction images, the *sky* is labelled with the blue color, while in ground truth it is labelled with black. It happened because the *sky* class does not exist in CARLA [20].

In Figure 4, we perform qualitative evaluation on Zed dataset. Our model generalized well to real-world data without any fine-tuning or parameters adjustment. We can see that objects such as *buildings*, *cars*, *poles* and *vegetations*

<sup>1</sup> $IoU = \frac{TP}{TP+FP+FN}$ , where TP is true positive, FP is false positive and FN is false negative pixels.

TABLE I  
 QUANTITATIVE EVALUATION ON CITYSCAPES DATASET. THE IOU METRIC IS SHOWN IN PERCENTAGE.

Object	FCN-8s	RefineNet	RecurrentParsing	DeepLab-v2(ResNet-101)	Ours
road	97.40	98.20	98.50	97.86	98.45
sidewalk	78.40	83.21	85.44	81.32	85.15
building	89.21	91.28	92.51	90.35	92.24
wall	34.93	47.78	54.41	48.77	47.10
fence	44.23	50.40	60.91	47.36	59.83
pole	47.41	56.11	60.17	49.57	63.12
traffic light	60.08	66.92	72.31	57.86	71.76
traffic sign	65.01	71.30	76.82	67.28	76.79
vegetation	91.41	92.28	93.10	91.85	93.22
terrain	69.29	70.32	71.58	69.43	71.80
sky	93.86	94.75	94.83	94.19	94.62
person	77.13	80.87	85.23	79.83	84.45
rider	51.41	63.28	68.96	59.84	65.66
car	92.62	94.51	95.70	93.71	95.36
truck	35.27	64.56	70.11	56.50	58.11
bus	48.57	76.07	86.54	67.49	73.70
train	46.54	64.27	75.49	57.45	61.99
motorcycle	51.56	62.20	68.30	57.66	66.82
bicycle	66.76	69.95	75.47	68.84	74.13
Mean IoU	65.3	73.6	78.2	70.4	75.4

TABLE II  
 QUANTITATIVE EVALUATION ON CARLA DATASET. THE IOU METRIC IS SHOWN IN PERCENTAGE.

Object	FCN-8s	RefineNet	RecurrentParsing	PSPNet	Ours
Buildings	57.86	77.05	72.34	71.84	79.08
Fences	14.04	28.53	20.47	25.01	21.78
Pedestrians	9.49	16.60	14.94	18.45	23.94
Poles	16.63	37.28	20.05	27.43	38.27
Roads	79.62	90.69	84.59	81.90	88.96
Sidewalks	26.83	66.14	22.47	10.11	48.45
Vegetation	69.16	70.81	69.99	71.49	68.87
Vehicles	32.73	42.35	58.68	62.93	64.86
Walls	2.49	9.67	4.17	3.43	8.78
Traffic Signs	11.11	26.90	30.21	30.69	27.65
Mean IoU	31.99	46.60	39.79	40.33	47.06

are segmented correctly even if they are cluttered. The failed case is in a wide area of *side walks*. As we can see in the 5<sup>th</sup> column, the wide *side walks* are segmented as a road. It possibly due to similar appearance and texture with the *road*.

### B. Quantitative

In Table I, we perform quantitative evaluation on Cityscapes [21]. We achieve 75.49% accuracy, which is comparable to other state-of-the-art methods. We gained 5% improvement over the baseline model DeepLab-v2(ResNet-101) [4]. Additionally, from the Table I, we can see that our approach achieves better performance for small objects such as *pole*, *traffic sign*, *person*, *car*, *terrain* and *vegetation*, while still having comparable results for other objects. For example in the *pole* class, we gain 13.5% improvement over the baseline DeepLab-v2(ResNet-101) [4] and 2.95% over RecurrentParsing [3].

In Table II, we perform quantitative evaluation on CARLA [20]. We perform inference on *validation* data. For a fair comparison, we compare our model with other publicly avail-

able Cityscapes-trained models without any fine-tuning or parameters adjustment. Note that our method achieves higher accuracies in several objects such as *buildings*, *pedestrians*, *poles* and *vehicles*. It may be worth mentioning that all methods perform poorly in segmenting *walls* where accuracies are less than 10%. One reason for this poor segmentation can be that the different shape and texture between the *walls* in CARLA 3D model and real-world object.

## V. CONCLUSIONS

In this paper, we proposed a network to address multi-scale objects in semantic segmentation. A novel combination of depth and multi-scale pyramid network specifically address the multi scale objects segmentation. Our evaluation demonstrated that the proposed network gained 5% improvement over the baseline RGB based method and achieve performance comparable to the state-of-the-art on Cityscapes [21]. Furthermore, we showed that our model is robust to other unknown test sets such as, synthetic images generated from CARLA [20] and on real world images captured using Zed stereo camera [33]. Future work includes training the

network with multiple GPUs to accommodate the batch size greater than one for faster training and more robust learning. Additionally, Bayesian learning [34] can increase the overall safety of Autonomous Vehicle (AV) by jointly learning the segmentation and uncertainties.

#### REFERENCES

- [1] E. Shelhamer, J. Long, and T. Darrell, "Fully convolutional networks for semantic segmentation," *IEEE transactions on Pattern Analysis and Machine Intelligence (PAMI)*, vol. 39, no. 4, pp. 640–651, 2017.
- [2] G. Lin, A. Milan, C. Shen, and I. D. Reid, "Refinenet: Multi-path refinement networks for high-resolution semantic segmentation," *arXiv preprint arXiv:1611.06612*, 2016.
- [3] S. Kong and C. C. Fowlkes, "Recurrent scene parsing with perspective understanding in the loop," *arXiv preprint arXiv:1705.07238*, 2017.
- [4] L. C. Chen, G. Papandreou, I. Kokkinos, K. Murphy, and A. L. Yuille, "Deeplab: Semantic image segmentation with deep convolutional nets, atrous convolution, and fully connected crfs," *IEEE transactions on Pattern Analysis and Machine Intelligence (PAMI)*, vol. PP, no. 99, pp. 1–1, 2017, ISSN: 0162-8828.
- [5] A. Krizhevsky, I. Sutskever, and G. E. Hinton, "Imagenet classification with deep convolutional neural networks," in *Advances in Neural Information Processing Systems (NIPS)*, 2012, pp. 1097–1105.
- [6] P. Sermanet, D. Eigen, X. Zhang, M. Mathieu, R. Fergus, and Y. LeCun, "Overfeat: Integrated recognition, localization and detection using convolutional networks," *arXiv preprint arXiv:1312.6229*, 2013.
- [7] K. Simonyan and A. Zisserman, "Very deep convolutional networks for large-scale image recognition," *arXiv preprint arXiv:1409.1556*, 2014.
- [8] C. Szegedy, W. Liu, Y. Jia, P. Sermanet, S. Reed, D. Anguelov, D. Erhan, V. Vanhoucke, and A. Rabinovich, "Going deeper with convolutions," in *Computer Vision and Pattern Recognition (CVPR)*, 2015, pp. 1–9.
- [9] R. Girshick, J. Donahue, T. Darrell, and J. Malik, "Rich feature hierarchies for accurate object detection and semantic segmentation," in *Computer Vision and Pattern Recognition (CVPR)*, 2014, pp. 580–587.
- [10] D. Erhan, C. Szegedy, A. Toshev, and D. Anguelov, "Scalable object detection using deep neural networks," in *Computer Vision and Pattern Recognition (CVPR)*, 2014, pp. 2147–2154.
- [11] S. Ren, K. He, R. Girshick, and J. Sun, "Faster r-cnn: Towards real-time object detection with region proposal networks," *IEEE transactions on Pattern Analysis and Machine Intelligence (PAMI)*, vol. 39, no. 6, pp. 1137–1149, 2017.
- [12] K. He, X. Zhang, S. Ren, and J. Sun, "Deep residual learning for image recognition," in *Computer Vision and Pattern Recognition (CVPR)*, 2016, pp. 770–778.
- [13] W. Liu, D. Anguelov, D. Erhan, C. Szegedy, S. Reed, C.-Y. Fu, and A. C. Berg, "Ssd: Single shot multi-box detector," in *European Conference on Computer Vision (ECCV)*, Springer, 2016, pp. 21–37.
- [14] B. Kayalibay, G. Jensen, and P. van der Smagt, "Cnn-based segmentation of medical imaging data," *arXiv preprint arXiv:1701.03056*, 2017.
- [15] H. Zhao, J. Shi, X. Qi, X. Wang, and J. Jia, "Pyramid scene parsing network," in *Computer Vision and Pattern Recognition (CVPR)*, 2017.
- [16] L. Chen, G. Papandreou, F. Schroff, and H. Adam, "Rethinking atrous convolution for semantic image segmentation," *arXiv preprint arXiv:1706.05587*, 2017.
- [17] G. Papandreou, I. Kokkinos, and P.-A. Savalle, "Modeling local and global deformations in deep learning: Epitomic convolution, multiple instance learning, and sliding window detection," in *Computer Vision and Pattern Recognition (CVPR)*, 2015, pp. 390–399.
- [18] L.-C. Chen, Y. Yang, J. Wang, W. Xu, and A. L. Yuille, "Attention to scale: Scale-aware semantic image segmentation," in *Computer Vision and Pattern Recognition (CVPR)*, 2016, pp. 3640–3649.
- [19] I. Kokkinos, "Pushing the boundaries of boundary detection using deep learning," *arXiv preprint arXiv:1511.07386*, 2015.
- [20] A. Dosovitskiy, G. Ros, F. Codevilla, A. Lopez, and V. Koltun, "CARLA: An open urban driving simulator," in *Proceedings of the 1st Annual Conference on Robot Learning*, 2017, pp. 1–16.
- [21] M. Cordts, M. Omran, S. Ramos, T. Rehfeld, M. Enzweiler, R. Benenson, U. Franke, S. Roth, and B. Schiele, "The cityscapes dataset for semantic urban scene understanding," in *Computer Vision and Pattern Recognition (CVPR)*, 2016.
- [22] D. Eigen and R. Fergus, "Predicting depth, surface normals and semantic labels with a common multi-scale convolutional architecture," *arXiv preprint arXiv:1409.1556*, 2014.
- [23] H. Noh, S. Hong, and B. Han, "Learning deconvolution network for semantic segmentation," in *International Conference on Computer Vision (ICCV)*, 2015, pp. 1520–1528.
- [24] P. Wang, P. Chen, Y. Yuan, D. Liu, Z. Huang, X. Hou, and G. W. Cottrell, "Understanding convolution for semantic segmentation," *arXiv preprint arXiv:1702.08502*, 2017.
- [25] C. Hazirbas, L. Ma, C. Domokos, and D. Cremers, "Fusenet: Incorporating depth into semantic segmentation via fusion-based cnn architecture," in *Asian Conference on Computer Vision (ACCV)*, 2016.
- [26] S.-J. Park, K.-S. Hong, and S. Lee, "Rdfnet: Rgb-d multi-level residual feature fusion for indoor semantic segmentation," in *International Conference on Computer Vision (ICCV)*, 2017.
- [27] Y. Cheng, R. Cai, Z. Li, X. Zhao, and K. Huang, "Locality-sensitive deconvolution networks with gated

- fusion for rgb-d indoor semantic segmentation,” in *Computer Vision and Pattern Recognition (CVPR)*, Institute of Electrical and Electronics Engineers, Inc., 2017.
- [28] K. He, X. Zhang, S. Ren, and J. Sun, “Deep residual learning for image recognition,” in *Computer Vision and Pattern Recognition (CVPR)*, 2016, pp. 770–778.
- [29] C. Couprie, C. Farabet, L. Najman, and Y. LeCun, “Indoor semantic segmentation using depth information,” *International Conference on Learning Representations (ICLR)*, 2013.
- [30] O. Russakovsky, J. Deng, H. Su, J. Krause, S. Satheesh, S. Ma, Z. Huang, A. Karpathy, A. Khosla, M. Bernstein, A. C. Berg, and L. Fei-Fei, “ImageNet Large Scale Visual Recognition Challenge,” *International Journal of Computer Vision (IJCV)*, vol. 115, no. 3, pp. 211–252, 2015.
- [31] A. Vedaldi and K. Lenc, “Matconvnet: Convolutional neural networks for matlab,” in *Proceedings of the 23rd ACM international conference on Multimedia*, ACM, 2015, pp. 689–692.
- [32] E. Games, *Unreal Engine 4*, “<https://www.unrealengine.com>”, Accessed 03-01-2018.
- [33] StereoLabs, *ZED Stereo camera*, “<https://www.stereolabs.com/zed/>”, Accessed: 2018-01-13.
- [34] R. McAllister, Y. Gal, A. Kendall, M. van der Wilk, A. Shah, R. Cipolla, and A. V. Weller, “Concrete problems for autonomous vehicle safety: Advantages of bayesian deep learning,” *International Joint Conferences on Artificial Intelligence, Inc.*, 2017.